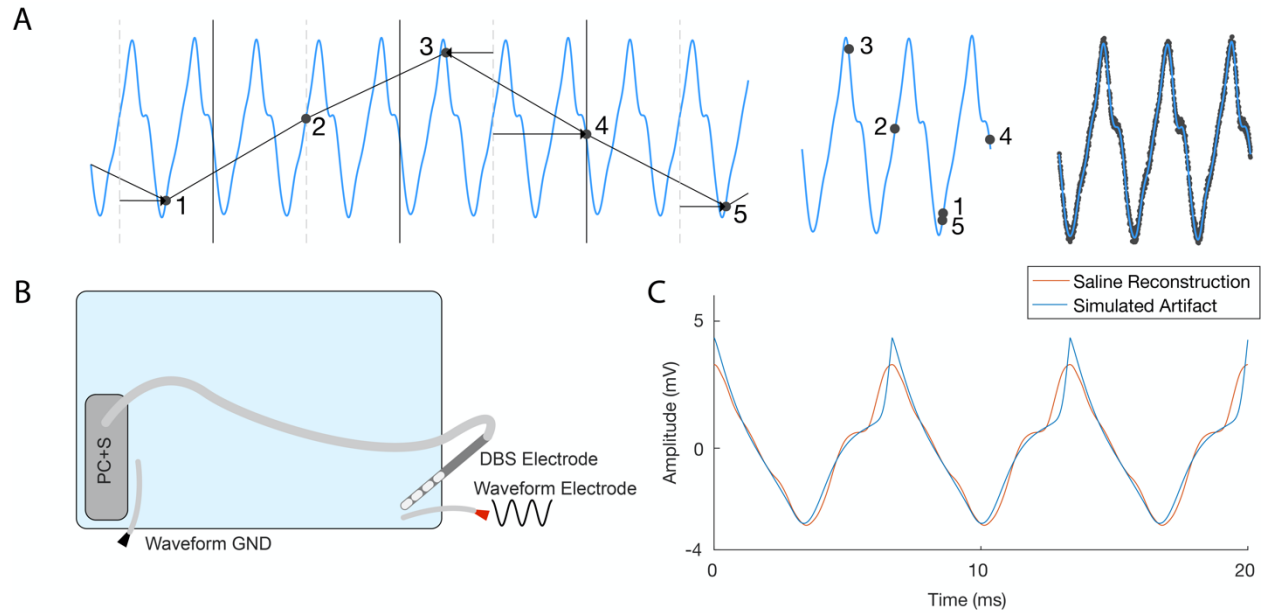


Cell Reports Methods, Volume 1

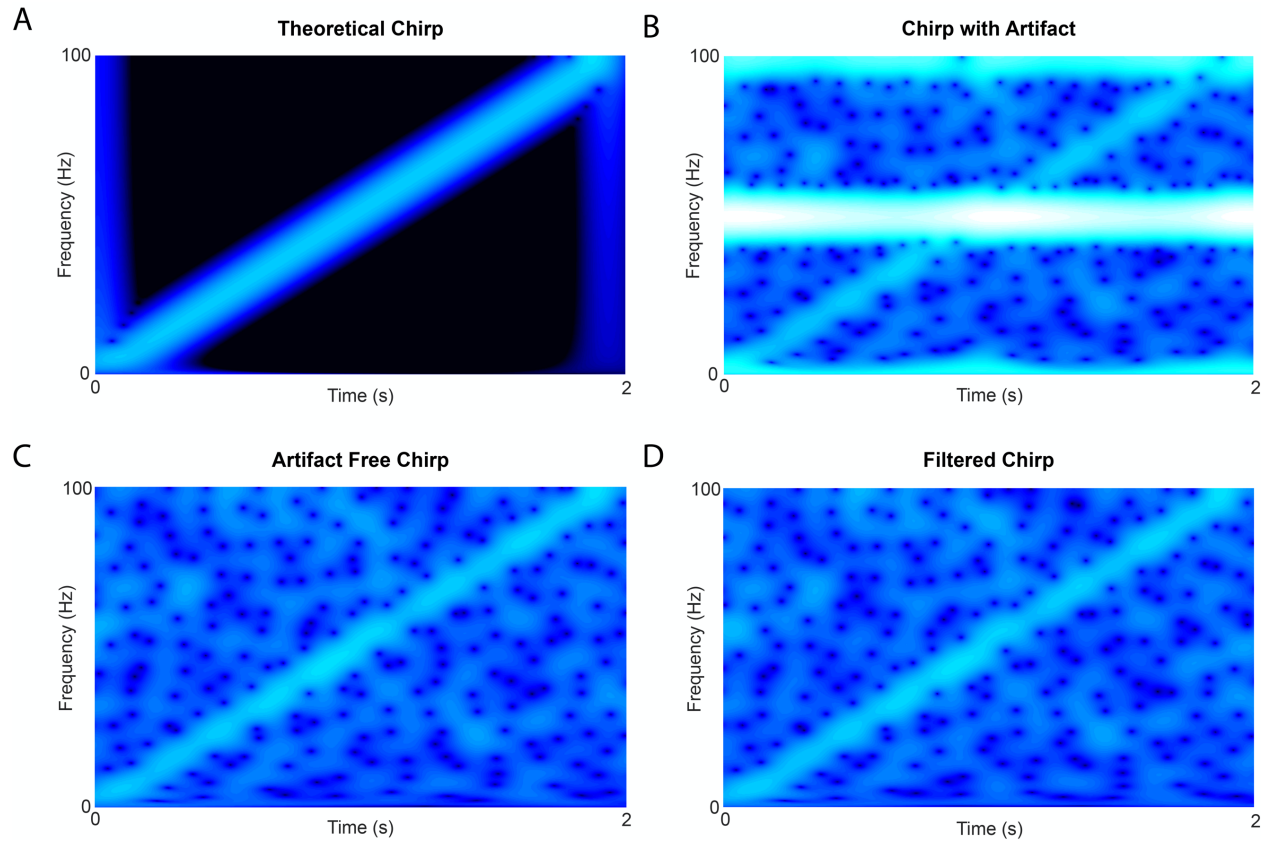
Supplemental information

**Uncovering biomarkers during therapeutic
neuromodulation with PARRM: Period-based
Artifact Reconstruction and Removal Method**

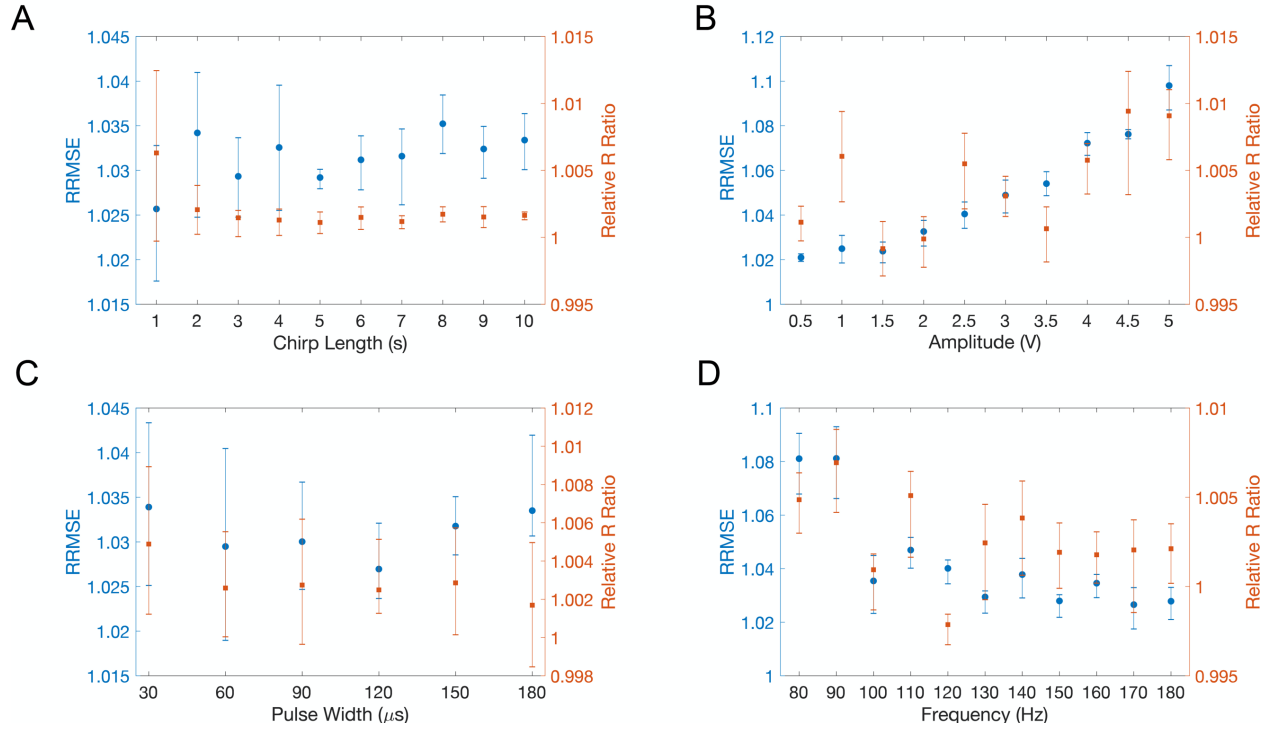
Evan M. Dastin-van Rijn, Nicole R. Provenza, Jonathan S. Calvert, Ro'ee Gilron, Anusha B. Allawala, Radu Darie, Sohail Syed, Evan Matteson, Gregory S. Vogt, Michelle Avendano-Ortega, Ana C. Vasquez, Nithya Ramakrishnan, Denise N. Oswald, Kelly R. Bijanki, Robert Wilt, Philip A. Starr, Sameer A. Sheth, Wayne K. Goodman, Matthew T. Harrison, and David A. Borton



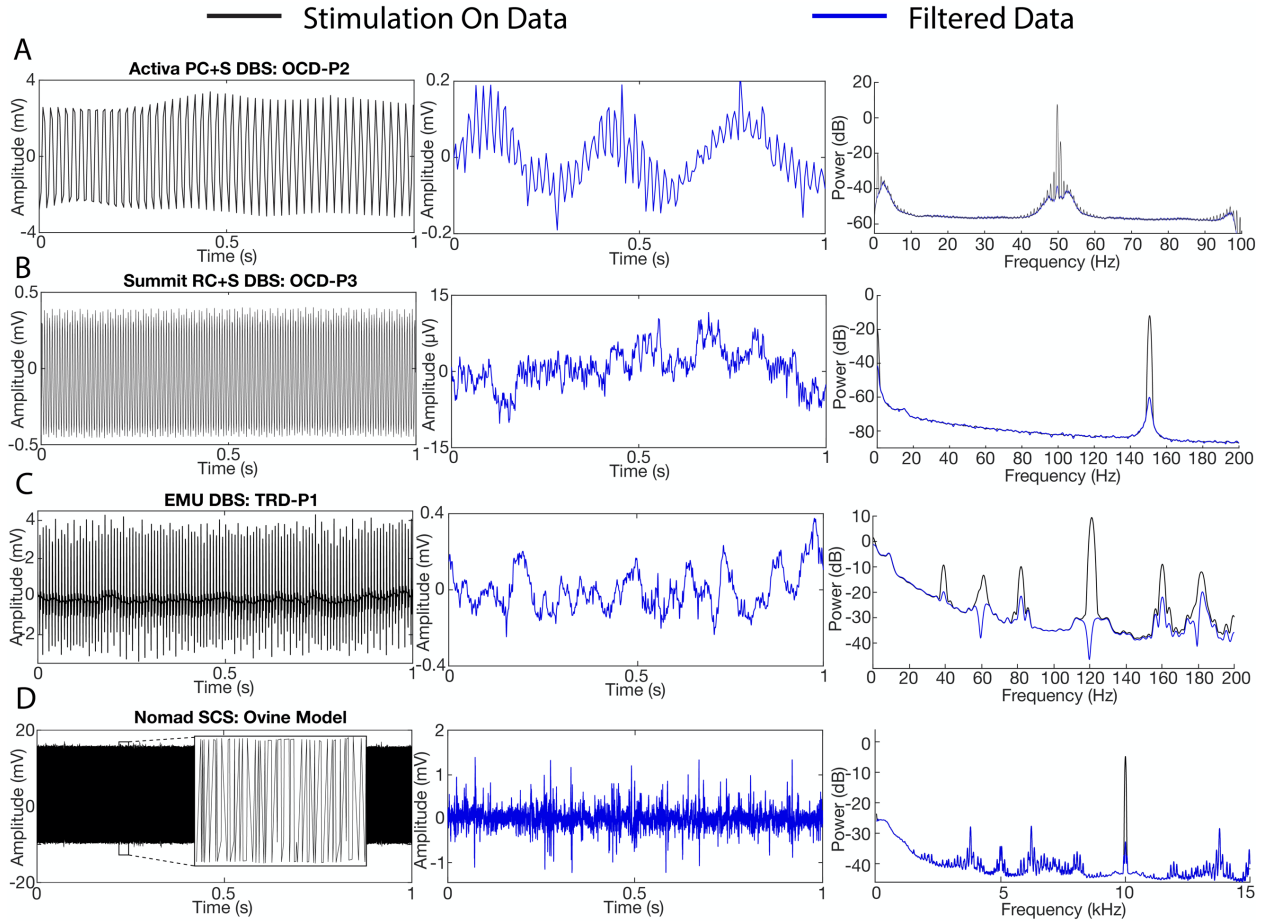
Supplemental Figure 1 (Related to STAR Methods and Figure 1): Supplemental methods figures. (A) Light blue trace indicates reconstruction of the estimated template waveform. Black trace indicates raw LFP sampled at 200 Hz. Black points indicate individual raw LFP samples. The distractor period results in a consolidated waveform consisting of multiple peaks and troughs. **(B)** The DBS lead and Activa PC+S case were immersed on opposite sides of a plastic container containing 1x phosphate buffered saline solution at room temperature. A platinum electrode connected to a waveform generator was placed adjacent to the stimulating electrode in order to simulate the neural signal appearing on the LFP. Single frequency oscillations were injected by the waveform generator alongside stimulation. **(C)** Simulated DBS waveform pulse train (blue) and a PARRM reconstructed waveform pulse train from saline experiments (orange).



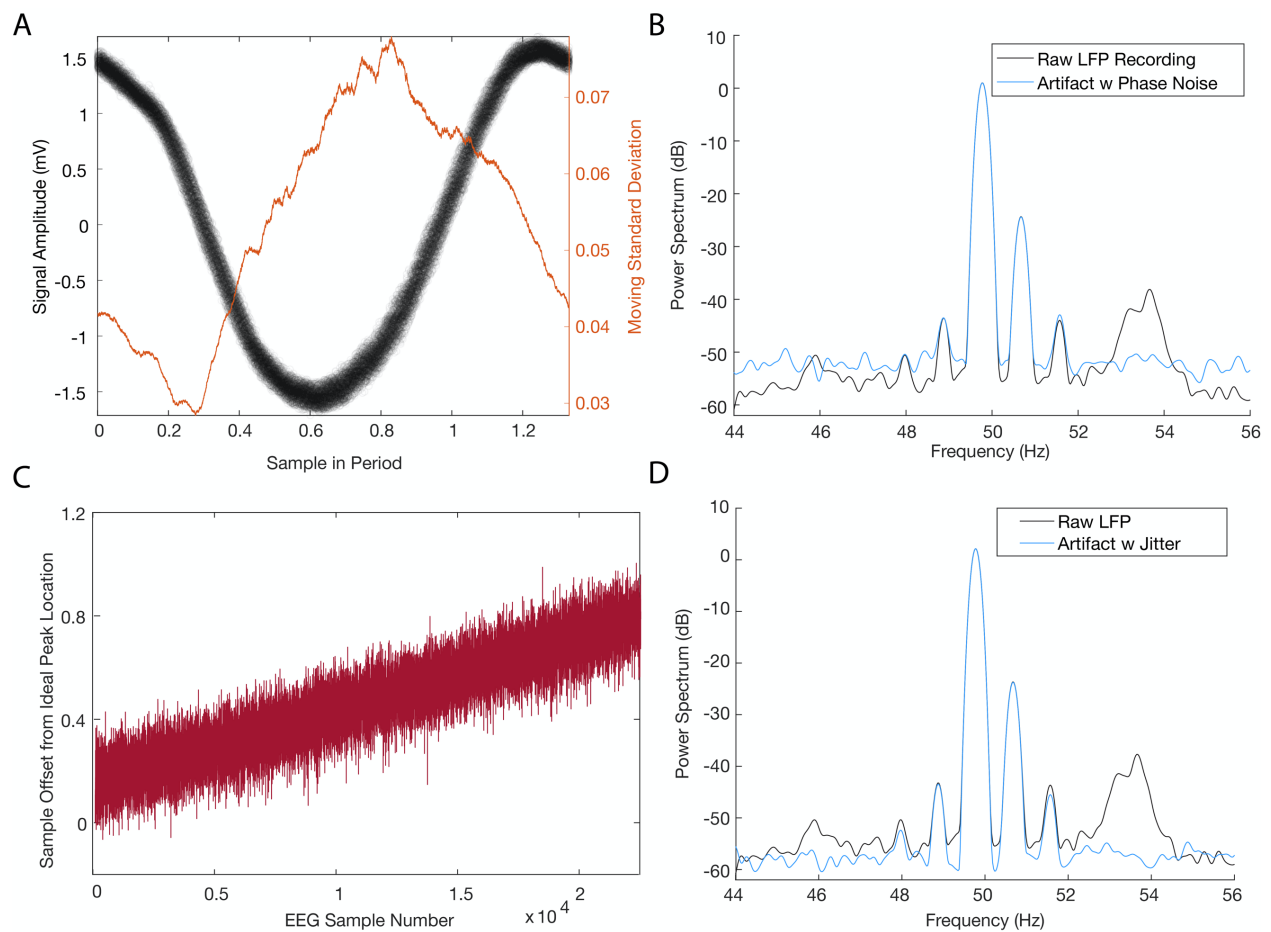
Supplemental Figure 2 (Related to Figure 3): Continuous wavelet transforms of simulated chirps. (A) Continuous wavelet transform of a theoretical chirp with no noise or stimulation. **(B)** Continuous wavelet transform of a chirp with noise and stimulation at 150 Hz. **(C)** Continuous wavelet transform of a chirp with noise and no stimulation. **(D)** Continuous wavelet transform of a chirp with noise and stimulation at 150 Hz, filtered using PARRM.



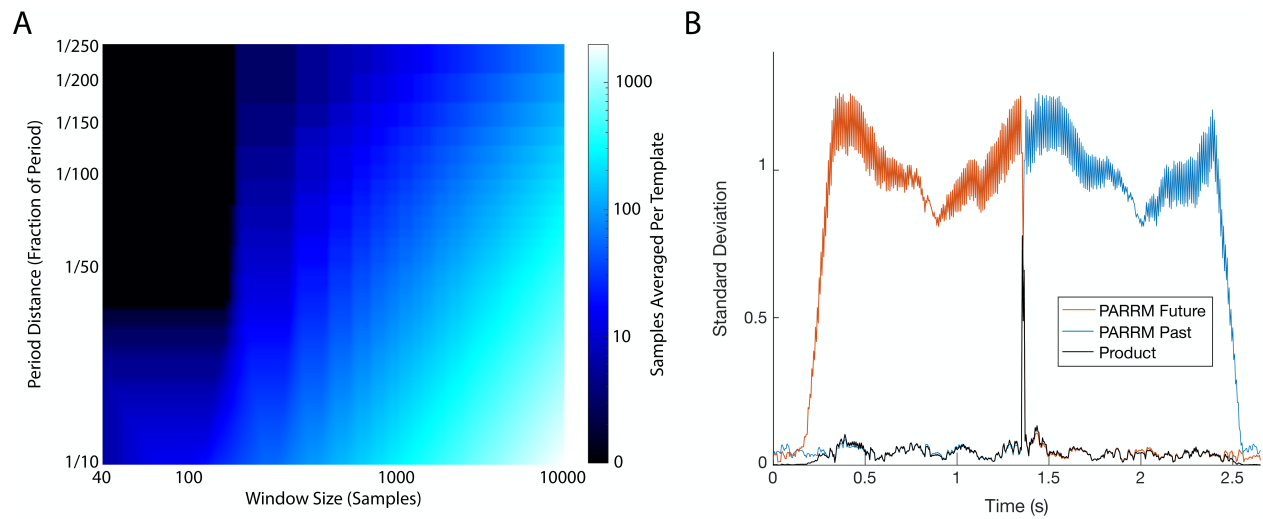
Supplemental Figure 3 (Related to Figure 3): Simulations show that PARRM is effective at a wide range of DBS parameters. Relative RMSE (time domain) and R Ratio (frequency domain) for variable (A) chirp length, (B) amplitude, (C) pulse width, and (D) frequency. Error bars show 95% confidence intervals on the median. Left Y axis in blue shows relative RRMSE. Right Y axis in orange shows Relative R Ratio.



Supplemental Figure 4 (Related to Figure 4): Additional Demonstration of PARRM in human participants with DBS and SCS in ovine model. (A-D) Raw time-voltage LFP trace, PARRM filtered time-voltage LFP trace, and average PSD before (black) and after (blue) PARRM filtering, collected during **(A)** 150 Hz stimulation sampled at 200 Hz using Activa PC+S in OCD-P2 left VC/VS, **(B)** 150.6 Hz stimulation sampled at 1000 Hz using Summit RC+S in OCD-P3 left VC/VS, **(C)** 120 Hz stimulation sampled at 2000 Hz in TRD-P1 right amygdala during a cognitive control task, **(D)** 10 kHz spinal stimulation sampled at 30 kHz in ovine model using Ripple Nomad



Supplemental Figure 5 (Related to Figure 4 and STAR Methods): Exploration of non-stationary oscillations leftover after PARRM in human data. (A) Black points show LFP samples from a single human Activa PC+S recording overlaid on a single period. Orange line shows the 1000 sample moving standard deviation of the residuals after PARRM overlaid on a single period. (B) Black line shows the power spectral density of the raw LFP signal. Blue line shows the power spectral density of the reconstructed artifact with the addition of phase noise (gaussian noise with zero mean and standard deviation equal to the corresponding phase on the orange trace). (C) Trace showing deviation of true DBS pulse time in EEG from pulse time predicted by PARRM as it varies across a recording. (D) Black line shows the power spectral density of the raw LFP signal. Blue line shows the power spectral density of the reconstructed artifact with the addition of the jitter sequence from panel C for each pulse.



Supplemental Figure 6 (Related to Figure 5): Additional details for real-time proof of concept. (A) Heat map of the number of samples averaged as a function of period distance (D_{period}) and half window size (N_{bins}). Darker blue indicates fewer samples averaged. Red point indicates the D_{period} and N_{bins} that were used for all analysis. **(B)** Moving standard deviation (5 sample window) using prediction from the left (blue), right (orange), and product of moving standard deviation from the left and right (black) illustrate method for identifying period jump in LFP recording. The peak of the product signifies the location of the period jump in LFP, and is used for aligning LFP to the corresponding point in EEG.